Peculiarities in Scattering Properties by Spherical Particles with Radial Anisotropy

Cheng-Wei Qiu[1] ***and Boris Luk'yanchuk***[2]

[1]National University of Singapore, 10 Kent Ridge Crescent, Singapore 119260. Email: eleqc@nus.edu.sg.

[2]Data Storage Institute, DSI Building, 5 Engineering Drive 1, Singapore 117608. Email: Boris_L@dsi.a-star.edu.sg.

Abstract

The role of anisotropy in plasmonic resonances and extraordinary scattering has been investigated in uncoated/coated spheres. It is shown that radial anisotropy may lead to great modifications in scattering efficiencies and field enhancement, elucidating the importance of anisotropies in the scattering control. The ability of "optical analog" of Landau damping is demonstrated for anisotropic spheres for the first time. Also, it is shown that by the suitable adjustment of the radius ratio in coated anisotropic spheres, one may make the anisotropic coated particle near transparent or invisible. This phenomenon is also explained in the effective medium theory, and physical insights are provided.

1. Introduction

It has been reported that the spherical or cylindrical cloak can be realized by the material with radial anisotropy using coordination transformation [1], which were primarily presented in the optics limit or static cases. Thus, an analytical method is necessary to exactly characterize the wave interaction and to provide more physical insight to the design process of cloaking structures. On the other hand, the nonlinear physics of the material studied in this report has been investigated [2], where the nonlinear enhancement in second-harmonic and induced third-harmonic generation is found to be much larger than that of the corresponding isotropic systems.

In medical applications and bio-engineering, the light scattering yields insight into the detail of interaction of embedded/injected bio-particles with the microwave and/or optical illuminations [3]. It helps, for example, to locate some abnormal proteins. A special interest presents the spherical particles with radial anisotropies. It is expected that molecules in spherical particles at least partially oriented with respect to the normal direction to the surface. Such orientational dynamics can be easily included into the theory considering the particle as a uniaxial anisotropic medium with the principal optic axis along with the local normal direction to the surface. The complex dielectric/magnetic tensorial components ϵ_n (μ_n) and ϵ_t (μ_t) correspond to the field vectors normal to, and tangential to the local surface (local optic axis [4]), respectively. This problem can be investigated on the basis of the analytical solution of Maxwell equations, which presents the extension of the Mie theory to the diffraction by an anisotropic sphere, including both electric and magnetic anisotropy ratio.

Some peculiarities in light scattering for isotropic materials were found recently for the case of weakly dissipating isotropic materials near plasmon resonance frequencies. For these materials, the classical Rayleigh scattering does not hold and can be replaced by anomalous light scattering [5]. This anomalous light scattering is associated with complex patterns of near- and far-fields in contrast to that of Rayleigh scattering. It also demonstrates an extraordinary scattering effect [6], which is similar to quantum scattering by a potential with quasi-discrete levels exhibiting Fano resonances [7]. Another interesting effect refers to active random isotropic media which support optical light enhancement [8]. Thus, the purpose of this paper is the analysis of the radial anisotropy effect upon the plasmonics and scattering properties on the basis of exact solution for light scattering by spherical particle with uniaxial anisotropy in both coated and uncoated cases.

2. Formulation and Field Expansion for Uncoated Spheres

In [9], it has been proved that in the radial anisotropic material the TE and TM waves are decoupled if off-axis elements are zero. Hence, solving the Maxwell equations using two Debye potentials [10], one has:

$$\frac{\epsilon_n}{\epsilon_t}\frac{\partial^2\Phi_{\rm TM}}{\partial r^2}+\frac{1}{r^2\sin\theta}\frac{\partial}{\partial\theta}(\sin\theta\frac{\partial\Phi_{\rm TM}}{\partial\theta})+\frac{1}{r^2\sin^2\theta}\frac{\partial^2\Phi_{\rm TM}}{\partial\phi^2}+\omega^2\mu_0\epsilon_0\mu_t\epsilon_n\Phi_{\rm TM}=0, \tag{1a}$$

$$\frac{\mu_n}{\mu_t}\frac{\partial^2\Phi_{\rm TE}}{\partial r^2}+\frac{1}{r^2\sin\theta}\frac{\partial}{\partial\theta}(\sin\theta\frac{\partial\Phi_{\rm TE}}{\partial\theta})+\frac{1}{r^2\sin^2\theta}\frac{\partial^2\Phi_{\rm TE}}{\partial\phi^2}+\omega^2\mu_0\epsilon_0\mu_n\epsilon_t\Phi_{\rm TE}=0 \tag{1b}$$

Here we define the parameters of anisotropy ratio: $\mathrm{A}_e=\epsilon_t/\epsilon_n$ (electric-type) and $\mathrm{A}_m=\mu_t/\mu_n$ (magnetic-type). For isotropic cases, Eqs. (1) and (1b) converts into usual wave equations. Electromagnetic fields can be expressed through those potentials (see *e.g.* [10]). Solving these equations with corresponding boundary conditions, one can find normalized scattering amplitudes a_l (electric) and b_l (magnetic)

$$a_l=\frac{\Re_l^{(a)}}{\Re_l^{(a)}+i\Im_l^{(a)}},\quad b_l=\frac{\Re_l^{(b)}}{\Re_l^{(b)}+i\Im_l^{(b)}} \tag{2}$$

where

$$\Re_l^{(a)}=n_t\psi_l'(q)\psi_{v_1}(n_tq)-\mu_t\psi_l(q)\psi_{v_1}'(n_tq),\quad \Im_l^{(a)}=n_t\chi_l'(q)\psi_{v_1}(n_tq)-\mu_t\chi_l(q)\psi_{v_1}'(n_tq) \tag{3a}$$

$$\Re_l^{(b)}=n_t\psi_l(q)\psi_{v_2}'(n_tq)-\mu_t\psi_l'(q)\psi_{v_2}(n_tq),\quad \Im_l^{(b)}=n_t\chi_l(q)\psi_{v_2}'(n_tq)-\mu_t\chi_l'(q)\psi_{v_2}(n_tq). \tag{3b}$$

Here $n_t=\sqrt{\epsilon_t\mu_t}$ is the complex refractive index, and functions $\psi_v(x)$ and $\chi_l(x)$ are given by $\psi_v(x)=\sqrt{\pi x/2}J_{v+1/2}(x)$ and $\chi_l(x)=\sqrt{\pi x/2}N_{l+1/2}(x)$, respectively. The primes indicate differentiation with respect to the entire argument. The value $q=k_0a$ presents the so called Mie size parameter, and a is the particle radius. One can see from these formulas that all the information about particle anisotropy is presented by the order of spherical Bessel functions [10], i.e., $v_1=\sqrt{n(n+1)\mathrm{A}_e+1/4}-1/2$ and $v_2=\sqrt{n(n+1)\mathrm{A}_m+1/4}-1/2$. The radius a of the anisotropic sphere is fixed at 30 μm. In practical detection problems, the so-called radar backscattering cross-section (RBSC) is of great interest. Those scattering efficiencies are basis for further numerical analysis.

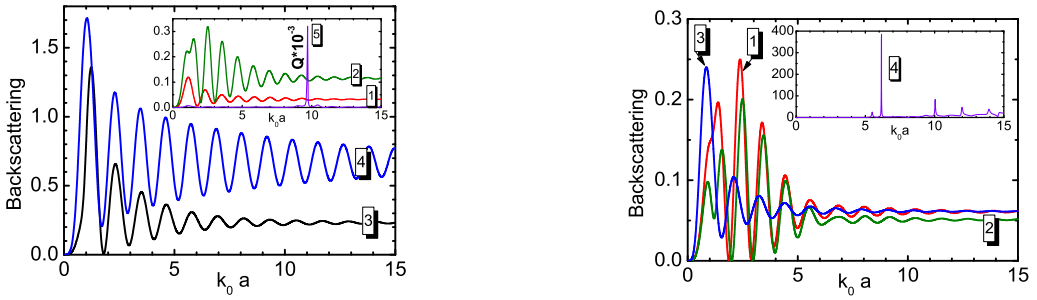

(a) (b)

Fig. 1. Normalized backscattering versus k_0a at the same scale of radial oscillation.
(a) only electric anisotropy ratio A_e is present: $\mu_n=\mu_t=1+0.2i$ and $\epsilon_n=2+0.6i$ are assumed for all curves; Curve 1 (red): $\epsilon_t=2+0.6i$ ($\mathrm{A}_e=1$); Curve 2 (olive): $\epsilon_t=4+1.2i$ ($\mathrm{A}_e=2$); Curve 3 (black): $\epsilon_t=8+2.4i$ ($\mathrm{A}_e=4$); Curve 4 (blue): $\epsilon_t=-4+1.2i$ ($\mathrm{A}_e=-1.67+1.1i$); Curve 5 (violet): $\epsilon_t=-4-1.2i$ ($\mathrm{A}_e=-2$). Red line corresponds to the isotropic case. In the curve 5, one can see light enhancement in anisotropic spheres with active transversal oscillation at 15.44THz (i.e., the size parameter at 9.7), and the amplitude of backscattering is shown with normalization factor of 10^{-3} (i.e. maximal amplitude is above 300).
(b) joint anisotropy ratios of A_e and A_m are present: the same radial oscillation is assumed $\epsilon_n=2+0.6i$ for all curves; Curve 1 (red): $\epsilon_t=4+1.2i$ ($\mathrm{A}_e=2$), $\mu_r=1+0.2i$, $\mu_t=1.5+0.3i$ ($\mathrm{A}_m=1.5$); Curve 2 (olive): $\epsilon_t=3.76+1.2i$ ($\mathrm{A}_e=2+0.4i$), $\mu_r=1+0.2i$, $\mu_t=1.5+0.3i$ ($\mathrm{A}_m=1.5$); Curve 3 (blue): $\epsilon_t=-4+1.2i$ ($\mathrm{A}_e=-1.67+1.1i$), $\mu_r=1+0.2i$, $\mu_t=-1.5+0.3i$ ($\mathrm{A}_m=-1.38+0.58i$); Curve 4 (violet): $\epsilon_t=-4-1.2i$ ($\mathrm{A}_e=-2$), $\mu_r=1+0.2i$, $\mu_t=-1.5-0.3i$ ($\mathrm{A}_m=-1.5$). For the last case, one can see light enhancement in active materials with negative refractive index at 9.8THz, i.e., size parameter at 6.16. Several enhanced backscatterings also exist at other frequencies.

In Fig. 1, we report the properties of backscattering normalized by the cross section (πa^2) with single anisotropy ratio (SAR) and joint anisotropy ratio (JAR). In Fig. 1(a), curves 1, 2, and 3 reveal the role of anisotropy in the scattering of normal anisotropic spheres, where limiting backscatterings are found for sufficiently high incident frequency. Interestingly, it is found that the backscattering would be significantly enhanced if the real part of electric SAR is negative. Also, it is noted that in the case such as Curve 4, the oscillation will exist in a wider band of frequency, resulting in no constant values. Given the physical size of the radius, one can sweep the incident frequency to differentiate those special molecules with negative

electric SAR from a molecular ensemble by the signal strength on the receivers. The inset in Fig. 1(a) further illustrates the sophisticated variation in a more detailed range. Of particular interest is the case of Curve 5, where light enhancement is observed and a small anisotropic object may be treated as if it is physically large. However, such giant enhancement is quite sensitive to the incident frequency.

Analogously, the oscillations in the backscattering for JAR are found to be convergent versus the size parameter. Comparing curve 1 with curve 3 in Fig. 1(b), one can see that the opposite signs in the real parts of transversal parameters (ϵ_t and μ_t) would lead to the same limiting value of backscattering, but the scattering patterns at small size parameters are dramatically modified. The enhanced light scattering of JAR seems in a more complex fashion than that of SAR. Multiple resonances can be found in JAR cases with the strongest one located at 9.8THz, the second strongest at 16.07THz, and some smaller ones.

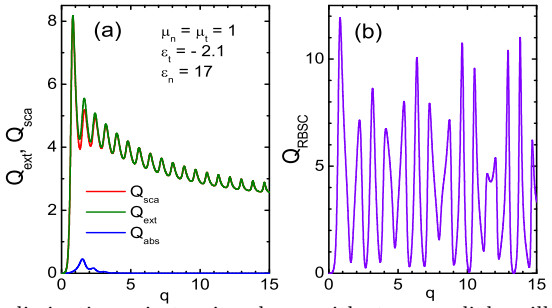

Fig. 2. Scattering efficiencies of nondissipative anisotropic spheres with strong radial oscillation where *optical analog* is found.

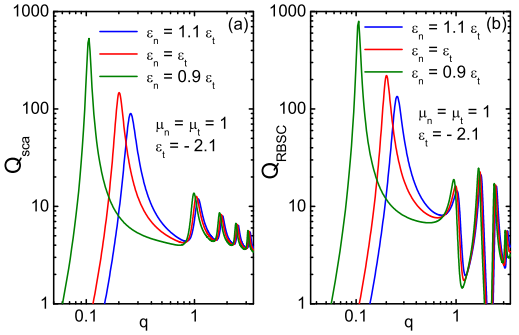

Fig. 3. Scattering efficiencies for nondissipative anisotropic spheres near surface-plasmon resonance.

The situation with different signs of ϵ_n and ϵ_t presents a special interest. In Fig. 2 one can see quite an unusual effect, when the particle is "plasmonic" ($\epsilon_t < -2$) in transversal direction and "dielectric" ($\epsilon_n > 1$) in radial direction. Although the material is nondissipative ($\mathrm{Im}[\epsilon] = 0$ for all cases), one can see $Q_{abs} \neq 0$ (with maximum near $q \approx 1.5$). This is not an artifact, and this effect is some kind of "optical analog" of Landau damping in a collisionless plasma [11]. The Landau damping occurs due to the energy exchange between a wave and particles in plasma, which accelerated or desselerated by the wave electric field. Formal mathematical reason for Landau damping is related to properties of some contour integral. Since we have no true dissipation in Fig. 2, it means that light energy is stored within the particle by reversible way and can be released [12], e.g. in the same fashion like plasma echo in collisionless plasma. Particles with radial anisotropy suggest a new idea for this light storage.

On the other hand, nondissipative anisotropic spheres near surface-plasmon resonances, with a slight anisotropy, is investigated. In such circumstance, it is found that the plasmon resonance is tunable by changing the velocities and directions of electron movements along radial oscillation direction. The red curve in Fig. 3 denotes the isotropic case near surface-plasmon resonance. However, even if the electron movement along radial oscillation is modified slightly, the scattering efficiencies will be varied drastically for small particles. Fig. 3 also shows that the electric anisotropy larger than unity (i.e., $A_e > 1$) favors the scattering enhancement particularly for nanoscaled particles. When the size parameter approaches to a sufficiently large value, the role of aniostropy becomes negligible.

3. Coated Anisotropic Spheres: Tunable Transparency and Enhancement

Assuming a coated structure where the core (c) and shell (s) are both radial anisotropic, the scattering coefficients can be obtained by applying boundary conditions (formulation will not be shown here). The role of the core-shell ratio in the extraordinary scattering is of particular interest as shown in Fig. 4. One may expect to tune the core-shell ratio to control the scattering at different modes. In Fig. 5(a), we find the local field is uniform in the core for isotropic case. The introduction of anisotropy as in Fig. 5(b) leads to large fluctation in local field, resulting in enhanced optical nonlinearity. The transparency conditions in Fig. 5 are determined from effective medium theory. The field outside the coated particles is nothing but the applied field, therefore the transparency mechanism is distinguished from Pendry's idea.

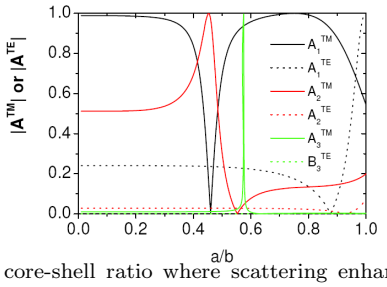

Fig. 4. Scattering coefficients versus the core-shell ratio where scattering enhancement or suppression occurs. The outer radius b is fixed at $0.2\lambda_0$. The parameters in the core: $\epsilon_{c,n} = 4$, $\epsilon_{c,t} = 2$, $\mu_{c,n} = \mu_{c,t} = 1$; and the parameters in the shell: $\epsilon_{s,n} = \epsilon_{s,t} = -3$, $\mu_{s,n} = 0.2$, $\mu_{s,t} = 0.5$.

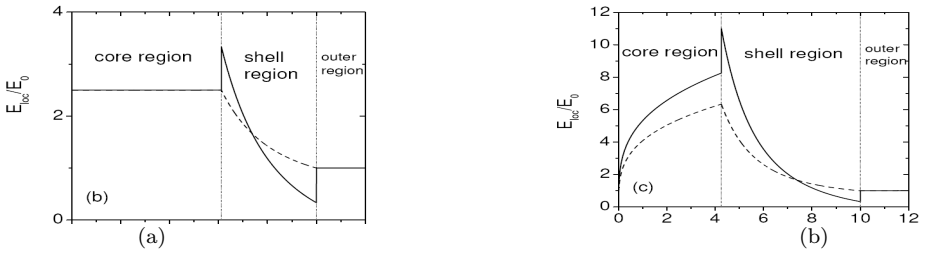

Fig. 5. Spatial dependence for the electric field throughout the coated sphere at transparency condition: (a) $\epsilon_{c,t} = \epsilon_{c,n} = 4$ (isotropic); and (b) $\epsilon_{c,t} = 6$ and $\epsilon_{c,n} = 4$. The outer radius $b = 0.2\lambda_0$. In the shell, $\epsilon_{s,n} = \epsilon_{s,t} = -3$. Materials in both shell and core are nonmagnetic. Solid curve: field parallel to the incident $\mathbf{E_0}$; dotted curve: perpendicular with $\mathbf{E_0}$.

4. Conclusions

Anomalous scattering of spherical particles with radial anisotropies are studied with physical insights by an exact solution to take into account the anisotropy effects. If the anisotropy and/or core-shell ratio are configured properly, small objects can be "observable" and (or) "transparent" to external detecting devices. Since abnormal membranes usually have much higher adhesive ability than normal ones, the theory proposed here would be very meaningful in the biomedical detection of those abnormal proteins if the future bio-technology makes it easier to arrange the desired deposits of such implanted orientational molecules so as to induce desirable anisotropy ratio.

References

[1] J. B. Pendry, D. Schurig, and D. R. Smith, Science **312**, 1780 (2006). D. Schurig, J. B. Pendry, and D. R. Smith, Opt. Express **14**, 9794 (2006). S. A. Cummer *et al.*, Phys. Rev. E **74**, 036621 (2006).
[2] L. Gao and X. P. Yu, Eur. Phys. J. B **55**, 403 (2007).
[3] M. F. Yanik *et al.*, Nature **432**, 822 (2004).
[4] C. F. Bohren and D. R. Huffman, *Absorption and Scattering of Light by Small Particles* (Wiley, New York, 1998).
[5] M. I. Tribelsky and B. S. Luk'yanchuk, Phys. Rev. Lett. **97**, 263902 (2006).
[6] B. S. Luk'yanchuk *et al.*, Appl. Phys. A **89**, 259 (2007).
[7] M. I. Tribelsky *et al.*, arXiv: 0708.1090v1 [cond-mat. soft] (8 Aug 2007).
[8] H. Cao *et al.*, Phys. Rev. Lett. **84**, 5584 (2000). P. Bermel *et al.*, Phys. Rev. B **73**, 165125 (2006).
[9] C. W. Qiu, L. W. Li, Q. Wu, and T. S. Yeo, IEEE Antennas Wirel. Propagat. Lett. **4**, 467 (2005).
[10] J. Roth and M. J. Digman, J. Opt. Soc. Am. **63**, 308 (1973). C. W. Qiu *et al.*, Phys. Rev. E **75**, 026609 (2007).
[11] L. D. Landau, *On electron plasma oscillations*, Sov. Phys. JETP **16**, 574 (1946) (in Russian).
[12] Z. M. Zhu, D. J. Gauthier, and R. W. Boyd, Science **318**, 1748 (2007).